Volume 1 | Number 1 | Jan 2013 | Pages 1–100

Integrative Biology

Interdisciplinary approaches for molecular and cellular life sciences
www.rsc.org/ibiology

ROYAL SOCIETY OF CHEMISTRY

This is an *Accepted Manuscript*, which has been through the Royal Society of Chemistry peer review process and has been accepted for publication.

Accepted Manuscripts are published online shortly after acceptance, before technical editing, formatting and proof reading. Using this free service, authors can make their results available to the community, in citable form, before we publish the edited article. We will replace this *Accepted Manuscript* with the edited and formatted *Advance Article* as soon as it is available.

You can find more information about *Accepted Manuscripts* in the Information for Authors.

Graphical and textual abstract

Using mathematical modeling and quantitative imaging, we demonstrate that the epidermal growth factor receptor is linearly transmitting extracellular information encoded in ligand concentrations into intracellular signals.
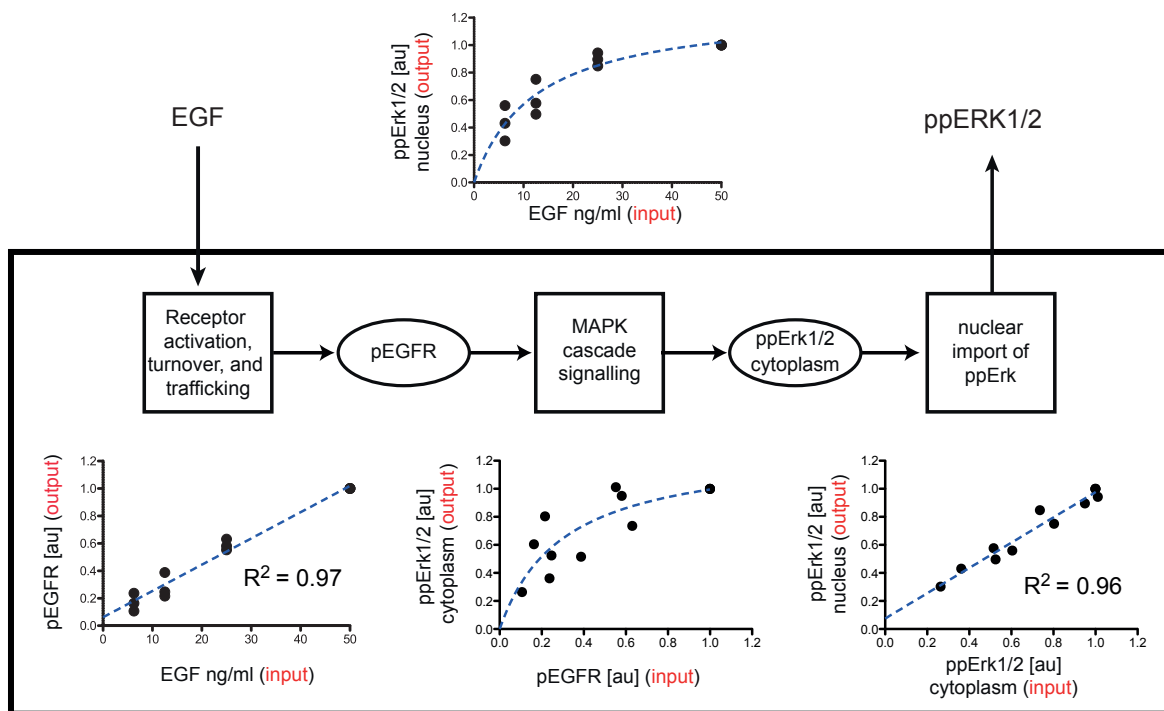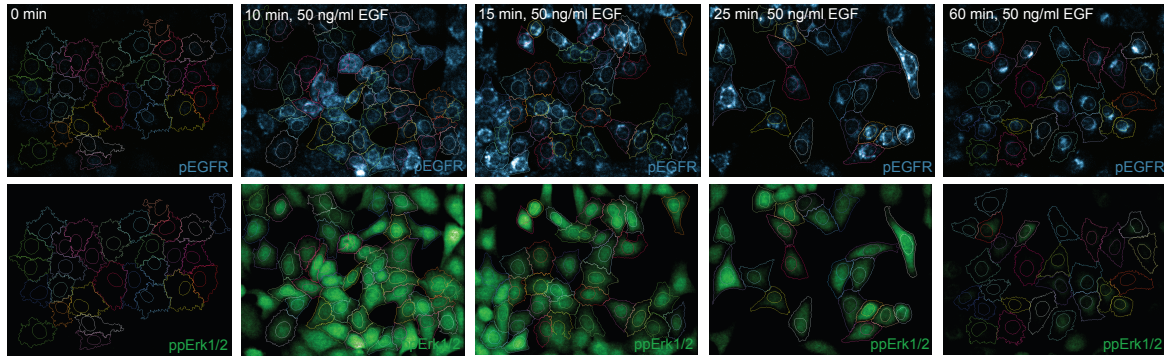
Insight, innovation, integration

We derived an analytical formula from nonlinear models of receptor signalling that have been used to model the signalling of the epidermal growth factor receptor (EGFR). The formula predicted that the cumulative EGFR signaling is linearly depending on the ligand concentration outside the cell. Quantitative imaging of HeLa cells suggests that the cumulative EGFR signaling indeed depends linearly on EGF concentration. Our mathematical approach therefore allows a simplified view on complex networks of receptor dynamics and describes the EGFR as a linear sensor of extracellular information encoded in ligand concentration.

ARTICLE TYPE

The EGFR demonstrates linear signal transmission[†]

Diego A. Oyarzún,[a] Jo L. Bramhall,[b] Fernando López-Caamal,[c] Frances M. Richards,[d] Duncan I. Jodrell,[bd] and Ben-Fillippo Krippendorff[*bd‡]

Cells sense information encoded in extracellular ligand concentrations and process it using intracellular signalling cascades. Using mathematical modelling and high-throughput imaging of individual cells, we studied how a transient extracellular growth factor signal is sensed by the epidermal growth factor receptor system, processed by downstream signalling, and transmitted to the nucleus. We found that transient epidermal growth factor signals are linearly translated into activated epidermal growth factor receptor integrated over time. This allows to generate a simplified model of receptor signaling where the receptor acts as a perfect sensor of extracellular information, while the nonlinear input-output relationship of EGF-EGFR triggered signalling is a consequence of the downstream MAPK cascade alone.

1 Introduction

Growth factor s control a number of cellular responses such as proliferation, differentiation, apoptosis and angiogenesis. Despite our comprehensive knowledge of some of the processes involved in growth factor sensing and signalling, we still lack a quantitative grasp of how they modulate the transmission of growth stimuli to the nucleus. One of the obstacles is the presence of regulatory feedback loops acting on both surface receptors and downstream signalling, which obscure the input-output relationship between ligand stimulus and the transmitted signal[1]. Moreover, growth factor signalling is a transient phenomenon because cells bind, internalize, and degrade ligand from the extracellular space. This causes receptor activation to weaken over the course of experiments, and thus extensive time course data are required to fully dissect the roles of individual processes.

The number of surface receptors available for binding is determined by receptor-related processes such as turnover, internalization, recycling and degradation[2]. As a consequence, cell surface receptors such as the epidermal growth factor receptor (EGFR) are increasingly being regarded as important

regulators of downstream signalling[1,3]. The number of EGFR molecules at the cell surface is regulated by a number of dynamical processes (Figure 1A): Newly produced receptors are translocated to the cell membrane, while receptors at the cell surface are constantly exchanged with intracellular endosomal compartments via clathrin-mediated endocytosis[4]. Further, internalized receptors can be recycled to the cell surface from early endosomes and late recycling compartments by fusing with the plasma membrane[5]. Endosomes that are not recycled eventually fuse with lysosomes which leads to proteolysis of attached receptors and bound ligands[6]. The level of free EGFR at the surface is therefore determined by the relative contributions of the individual trafficking and degradation processes.

Ligands in the extracellular space also influence the fate of receptors at the cell membrane. Binding of ligands to the EGFR, for example, induces dimerization and autophosphorylation of intracellular residues[7]. These phosphorylations are responsible for the activation of different downstream signalling cascades, most prominently the mitogen-activated protein kinase (MAPK) cascade, composed of Ras-Raf-Mek-Erk, and the PI3K-Akt cascade[8]. At the same time, ligand binding perturbs the balance of the individual receptor trafficking processes by increasing the internalization rate of EGFR[9,10]. Via this mechanism, receptor activation can potentially exert a negative feedback effect by increasing internalisation, and eventually degradation, of receptors and ligands in lysosomes[1,11,12].

A number of mathematical models for the EGFR system have shed new light on the design principles underpinning growth factor signalling. One of the first examples was the steady state model of EGFR activation and trafficking by Wi-

† Electronic Supplementary Information (ESI) available: [details of any supplementary information available should be included here]. See DOI: 10.1039/b000000x/

a Department of Mathematics, Imperial College London, UK

b Department of Oncology, University of Cambridge, UK

c Hamilton Institute, National University of Ireland, Maynooth, Ireland

d Pharmacology & Drug Development Group, Cancer Research UK Cambridge Institute, UK

‡ Present address: Roche Pharmaceutical Research and Early Development, Pharmaceutical Science, Roche Innovation Center Basel, Grenzacherstrasse 124, 4070 Basel, Switzerland, Tel: +41616889732; E-mail: ben-fillippo.krippendorff@roche.com
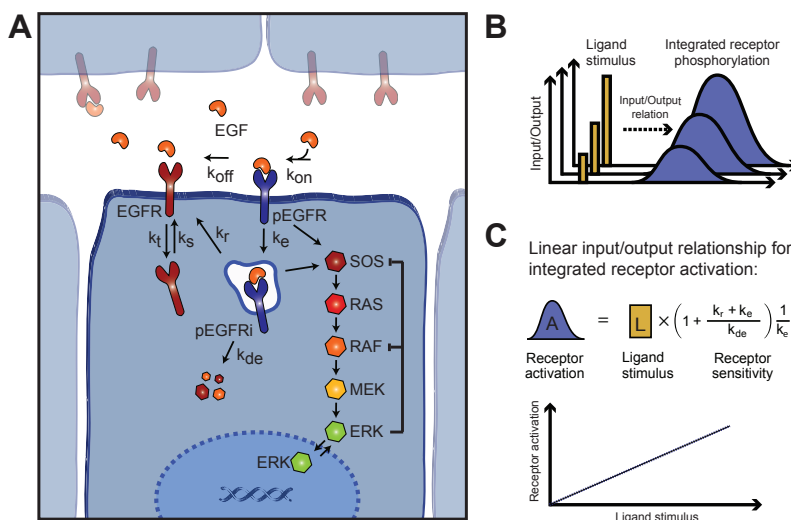
Fig. 1 Linear signal transmission in a model for epidermal growth factor receptor (EGFR) binding, turnover and trafficking. **A)** EGF -induced signalling comprises ligand sensing by the EGFR on the cell surface, transmission of the sensed signal via the MAPK cascade, and nuclear import of active ERK. Extracellular EGF binds to free EGFR, triggering its dimerization and subsequent phosphorylation (pEGFR). Active receptors trigger the activation of the MAPK cascade and also get internalized by endosomes (pEGFRi). The endosomes are either degraded or recycled back to the cell surface. The MAPK cascade results in ppErk in the cytoplasm, which is finally imported into the nucleus to induce transcriptional changes. Eq. (1) is an ODE model of receptor binding, turnover and trafficking; the parameters are described in Table S1 in the Supplementary Information. **B)** Here we investigate the input-output relationship between a certain bolus extracellular stimulus (EGF concentration) and the resulting EGFR phosphorylation integrated over time (area under the activation curve). **C)** The model predicts a linear input/output relationship between ligand concentration and integrated receptor phosphorylation.

ley et al. [13]. EGFR models have also proven useful to describe other receptor systems subject to the same processes (binding, internalization and recycling), but with parameter values that describe particular instances of a core network model [14]. Increasingly detailed models have been recently built to capture the mechanistic processes that control the input-output relationship of the EGFR system [15].

Here we report our studies on the relationship between extracellular ligand concentration and processes influencing EGFR signaling, such as ligand binding and receptor trafficking. We describe a previously unreported feature of EGFR signalling: its ability to linearly transmit extracellular ligand cues into cytoplasmic receptor activation. Using a combination of mathematical modelling, analysis and high-throughput imaging, we present evidence suggesting that receptor trafficking produces a linear input-output relationship between initial ligand concentration and the cumulative receptor phosphorylation. The cytoplasmic signal in turn acts as an input to subsequent signalling cascades that cause signal saturation.

2   Materials and methods

Cell Culture

The human cervical carcinoma HeLa cells were obtained from CRUK Cambridge Institute and were authenticated by STR genotyping as well as tested negative for mycoplasma. These cells were maintained with Dulbecco's Modified Eagle Medium (DMEM) (Life Technologies Ltd, Paisley, UK) supplemented with 10% Fetal Calf Serum (FCS) (Life Technologies Ltd, Paisley, UK) at 37°C in a humidified atmosphere of 5% CO2 in atmospheric O2 levels.

Immunofluorescence

Immunofluorescence was performed in ibidi 96-well plates (ibidi GmbH, Germany); cells were incubated at 37°C for 24 h. After 24 h, the media was replaced with media containing no serum and incubated for a further 16h at 37°C. The cells were stimulated with 0, 6.25, 12.5, 25 and 50 ng/mL EGF (#01-101, Millipore, USA) at various time points, fixed with 4% paraformaldehyde in PBS and blocked with PBS/1% BSA (w/v)/0.1% saponin (w/v) (PBS/B/S) and 5% goat serum (v/v) (GS) for 1h. Cells were incubated for 16 h at 4°C with pEGFR (rabbit poly clonal anti-pEGFR Tyr1068, #3777 Ab,

1:600; Cell Signalling Technologies) and ppErk1/2 (mouse polyclonal anti-ppErk1/2 T185,Y187 T202 Y204, #ab50011 Ab, 1:500; Abcam). The plates were washed with PBS/B/S + 1% GS five times and incubated with secondary antibodies antimouse IgG Alexa Fluor 488 (44085 Ab, 1:1000; Cell Signalling Technologies), antirabbit IgG Alexa Fluor 647 (44145 Ab, 1:1000; Cell Signalling Technologies) and DAPI (Invitrogen) for 1 h in the dark at room temperature. The plates were washed with PBS/B/S + 1% GS five times and stored in PBS at 4°C in the dark until analysis.

High-throughput imaging

Quantitative imaging was performed by acquiring pictures of each well of the 96-well plate using the iCys Research Imaging Cytometer (CompuCyte, MA, USA) using 40x magnification and lasers 405 nm, 488 nm, and 633 nm. This microscope is purpose built for the quantification of fluorescent signals in cells and is widely used for Laser Scanning Cytometry. Analysis of the field images using the Columbus software (version 2.3, PerkinElmer) and Matlab (version 7.14, Mathworks). In each plate, two wells for each timepoint and treatment were measured. The data was then normalised in Prism (version 5, Graphpad) on each plate by defining the signal seen in the unstimulated wells as zero and the highest signal measured on the plate as one. Detailed information about the quantification on the field images and the data analysis pipeline can be found Section S2 of the Supplementary Information.

Mathematical modelling and analysis

The details of the mathematical methods can be found in the Supplementary Information. Extensions of our method to compute the time-integrals of species concentrations in nonlinear reaction-diffusion models can be found in[23].

3   Results

Exact computation of the integrated response in signalling networks

To investigate the relation between EGFR trafficking and receptor activation, we first built an Ordinary Differential Equation (ODE) model for ligand binding, receptor trafficking, and turnover. The model comprises the receptor processes in Figure 1A and describes the dynamic response of ligand, free re-

ceptors, active receptors and endosomes :

$$
\begin{aligned}
\frac{dL}{dt} &= f(t) - k_{on}R \cdot L + k_{off}C + k_{r}C_{int}, \\
\frac{dR}{dt} &= k_{s} - k_{t}R - k_{on}R \cdot L + k_{off}C + k_{r}C_{int}, \\
\frac{dC}{dt} &= k_{on}R \cdot L - k_{off}C - k_{e}C, \\
\frac{dC_{int}}{dt} &= k_{e}C - k_{r}C_{int} - k_{de}C_{int}.
\end{aligned}
\tag{1}
$$

Here L is the concentration of EGF ligand supplied to the medium at a rate $f(t)$, R is the concentration of free receptors (EGFR), C is the concentration of phosphorylated receptors (pEGFR), and C_{int} is the concentration of endosomes (pEGFRi). The parameters of the model are described in Table S1 in the Supplementary Information. This model has been widely used to describe the EGFR and other receptor tyrosine kinases systems such as the HER2[14,16–19], as well as cytokine receptors such as the erythropoietin receptor (EpoR) and the Interleukin 3 receptor[14,20].

We focused on the relationship between the ligand concentration (dose) and the area under the receptor activation curve (see Figure 1B). This time-integral represents the cumulative activation of the receptor over time and depends on the duration and peak of the activation. The area under the activation curve is a good measure of a transient response and has proven useful to study signaling cascades[21,22], reaction-diffusion systems[23], cell surface receptors[20], and was also found to link ERK activation with DNA synthesis[24].

To study the input-output relationships of cellular signaling models, simulations are typically used to obtain sensitivities of outputs on the different model components. Conclusions drawn from simulation-based studies , however, can be depend strongly on the specific parameter values used in the simulations. Moreover, model parameters are typically subject to high uncertainty due to limited quantitative knowledge of the reaction kinetics and the limited datasets available for parameter estimation.

We here present an analytic approach to quantify the input-output relationship of cellular signaling models. To derive conclusions that are independent of the parameter values, we sought to analytically solve the time-integrals of the activated receptors as a function of the parameters. Signaling networks, however, display highly nonlinear dynamics and thus exact model solutions are hard (if not impossible) to obtain. We developed a mathematical approach to obtain exact formulae for the integrated response of signalling networks under external inputs.

We considered a signalling network with m reactions and n

chemical species

$$\sum_{i=1}^{n} \alpha_{ij} s_i \overset{v_j}{\longleftrightarrow} \sum_{i=1}^{n} \beta_{ij} s_i, \quad j = 1, 2, \dots, m,$$
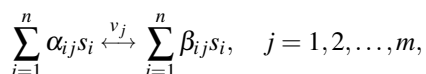
for $j = 1, 2, \dots, m$. The variables s_i represent species concentrations, whereas α_{ij} and β_{ij} are the stoichiometric coefficients of species s_i in reaction v_j. To account for the interaction between the network and its environment, the species may be supplied to or consumed from the network at a rate u_i. An ODE model for the network reads

$$\frac{\mathrm{d}s}{\mathrm{d}t} = Nv(s) + Du,$$

where s is the vector of species concentrations, v is the vector of reaction rates, and u is the vector of external stimuli. The stoichiometric matrix N has entries $N_{ij} = \beta_{ij} - \alpha_{ij}$; species s_i is consumed or produced in reaction v_j whenever $N_{ij} < 0$ or $N_{ij} > 0$. We modelled the effect of the stimuli with the matrix D, which determines which species are affected by stimulus u_i (for example, to model an influx u_i of species s_i, we choose the j$^{\text{th}}$ column of D to have a 1 in its i$^{\text{th}}$ entry and zeros elsewhere). We consider stimuli signals of the form $u(t) = \bar{u} + \delta(t)$, with $\bar{u}$ being a constant stimuli and $\delta(t)$ being a transient signal that vanishes to zero after sufficiently long time. After the transient stimuli have vanished, we assume that the network reaches a unique and globally stable steady state $\bar{s}$ that matches the pre-stimulus steady state concentrations.

We obtained conditions on the network structure and reaction kinetics under which the integrated response of some of the species can be exactly computed from the formula:

$$\int_0^{\infty} (s_i - \bar{s}_i) \, \mathrm{d}t = f(p) \left(\tilde{s}_0 + u_T \right), \tag{2}$$

where $\bar{s}_i$ is the steady state concentration of s_i, $f(p)$ is a nonlinear function of the model parameters (including for example, the stoichiometry and kinetic parameters), $\tilde{s}_0 = s_i(0) - \bar{s}_i$ is the initial deviation of s_i from its steady state concentration, and $u_T = \int_0^{\infty} \delta \, \mathrm{d}t$ is the net concentration of species supplied to the network by the transient signal $\delta(t)$. The formula in eq. (2) holds under conditions that depend on the stoichiometry and nonlinear kinetics, and describes the integrated response of s_i in terms of the kinetic parameters, initial concentrations and the external stimuli. The derivation of the network conditions can be found in Sections S1.1-S1.2 of the Supplementary Information; further extensions and interpretations of these conditions for spatiotemporal models can be found in [23].

The EGFR displays linear signal transmission

Using our approach in the model for EGFR binding, turnover

and trafficking (Figure 1A), we found a simple linear input-output formula for the integrated receptor activation A:

$$A = \frac{1}{k_{\text{e}}} \left(1 + \frac{k_{\text{e}} + k_{\text{r}}}{k_{\text{de}}} \right) L_{\text{total}}, \tag{3}$$

where L_{total} is the total concentration of ligand supplied to the extracellular medium. The linear relationship is illustrated in Figure 1B–C and its derivation can be found in section S1.3 in the Supplementary Information. For the considered model, the formula in eq. (3) is an exact description of the cumulative concentration of membrane-bound and internalised active receptors (pEGFR and pEGFRi in Figure 1A) following a ligand stimulus; given model-specific parameter values, the formula can be used to quantitatively predict the magnitude of receptor activation. The expression in (3) suggests that not all the processes affect the cumulative activation. In particular, receptor turnover (determined by k_{t} and k_{s}) as well as ligand binding (k_{on} and k_{off}) cancel out and do not affect the activation integrated over time. The formula for A therefore predicts that, despite the nonlinearities introduced by the limited amount of receptor available for binding, the integrated receptor activation scales linearly with the ligand concentration.

We then asked whether the predicted linearity is a consequence of the specific binding kinetics assumed in the model (described as a bimolecular mass action process), and consequently computed the integrated activation for a generic family of binding kinetics. We found that linear signal transmission seems to be independent of the binding mechanism (see Section S1.4 in the Supplementary Information) and furthermore, it should appear even when assuming saturable or cooperative binding.

Our result suggests that cumulative activation of EGFR depends on the trafficking processes, that is, on the interplay between receptor recycling, internalization and breakdown. Receptor trafficking therefore seems to be the key process enabling a broad dynamic range in EGFR signal transmission. Since this principle emerges independently of specific parameter values, it also suggests that it could be a robust property conserved across the family of receptors subject to trafficking, binding and turnover processes.

To experimentally test our theoretical prediction, we measured the temporal response of EGF-triggered phosphorylation of EGFR in HeLa cells with high-throughput quantitative immunofluorescence imaging. We first determined the range of EGFR concentrations that resulted in measurable EGFR phosphorylation (details in the Supplementary Information). For the batch of EGF used, EGFR phosphorylation was measured for concentrations above 10 ng/ml using quantitative Western Blotting. Next, we serum starved HeLa cells to eliminate all growth factor mediated EGFR phosphorylation and then stimulated the cells with 6.25 to 50 ng/ml EGF.
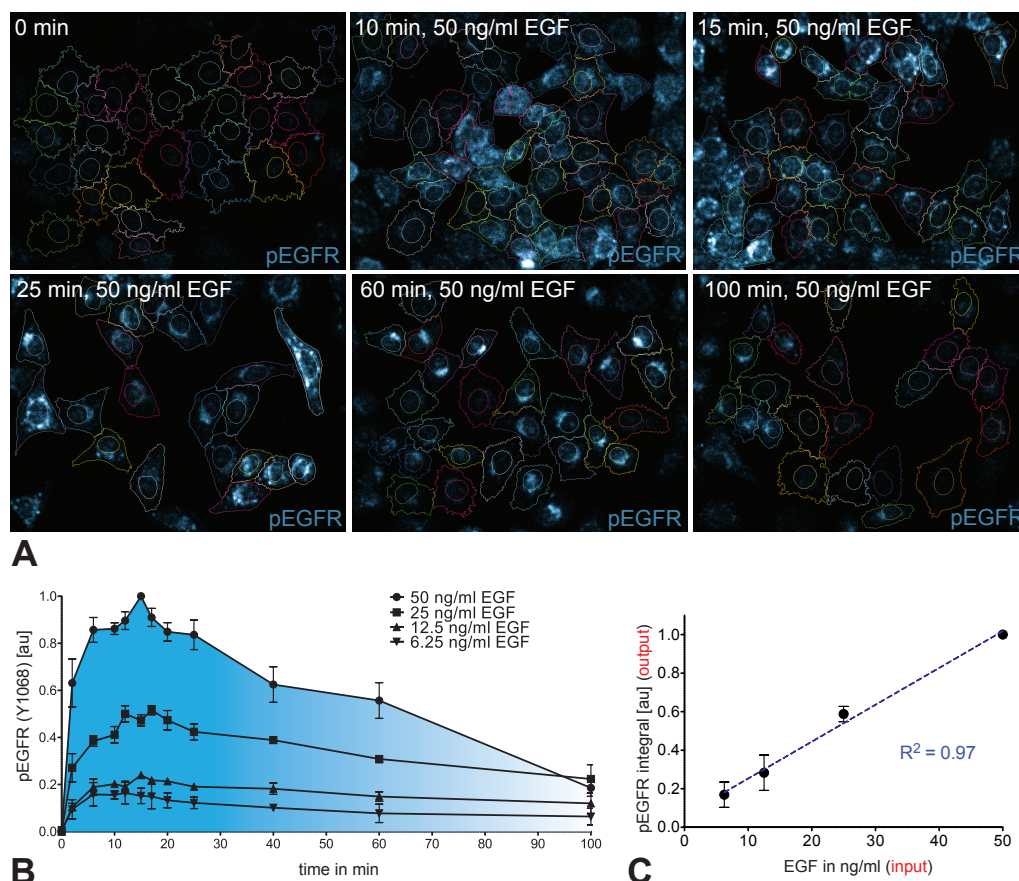
Fig. 2 Transient activation of EGFR after stimulation of Hela cells with different concentrations of EGF. **A)** Serum starved Hela cells were stimulated with 50 ng/ml EGF for different times; the chosen concentrations are within the range where EGFR phosphorylation was detectable via western blot, see Supplementary Material. Cells were stained for DNA (DAPI) and pEGFR (Y1068) for imaging. Individual cells were identified based on DAPI staining and segmentation of the cytoplasmic staining as described in the Material and Methods section. The EGF concentrations for stimulation were determined by Western Blotting (Supplementary Figure S4). **B)** Cytoplasmic and membrane staining was quantified for ca. 1500 individual cells per well. For each 96-well plate the data was normalised by dividing by the highest value per well observed over all timepoints. Data represents the mean of all quantified cells, while error bars represent the standard error between three biological replicates. **C)** Measured pEGFR signal was integrated over time for the indicated concentrations of EGF. Integrated activation was normalised to the highest value observed for the different ligand concentrations on the plate. Error bars represent the standard error between three biological replicates. The dashed line is a linear fit of the data.

The imaging approach was used to determine the signal in different compartments of the cell. Further, single-cell imaging allows to derive a mean value of thousands of individual measurements. We scanned 96-well plates using a laser cytometer and segmented individual cells from the collected images (Figure 2A and details in Materials and Methods). We then quantified in each cell the level of EGFR phosphorylation at Y1068, which is crucial for downstream signalling and activation of the MAPK cascade resulting in Erk1/2 activation[9,25].

Mean EGFR phosphorylation peaked at around 15 min after EGF stimulation (Figure 2B), followed by a slow reduction of pEGFR signal corresponding to the internalization and degradation of activated receptor after around 5-20 min[26]. At later timepoints localised intracellular staining close to the nucleus was apparent, most likely representing trafficking of EGFR to the endoplasmatic reticulum. We integrated the mean phosphorylation level of all measured cells over the timescale of the experiment (0-100 minutes). In agreement with our theoretical predictions, the integrated response of pEGFR was found to be proportional to the initial EGF concentrations (Figure 2C), confirming that the EGFR linearly translates the extracellular EGF into an integrated response of receptor phosphorylation.

We suggest that linear signal transmission may be a consequence of a negative feedback exerted by receptor trafficking. Processes such as receptor endocytosis, recycling and degradation processes determine receptor activation integrated over time and hence limit receptor signaling. As a consequence, the model suggests that in cancer cells mutations that reduce receptor internalization and degradation could be especially beneficial to maximize stimulation from a limited supply of growth factors. This could be another aspect of the important role of mutations that modify receptor trafficking in cancer[27-30].

The MAPK cascade limits the dynamic range of signal transmission

Next we investigated how the linear signal of activated EGFR is transmitted into the cytoplasm and nucleus. In addition to pEGFR, we measured activated Erk1/2 in the cytoplasm and the nucleus (Figure 4A) using an additional antibody specific to double phosphorylated Erk1/2. The high-throughput imaging approach hence allowed us to determine pEGFR and ppERK1/2 levels for individual cells.

We found that the time profile of Erk activation follows a similar shape to that of receptor activation, but reaches its peak earlier at around 8-10 min and drops sharper afterwards (Figure 3B). This quick response of Erk1/2 upon upstream receptor activation has been previously ascribed to the ultrasensitive behaviour arising from double phosphorylation of ERK

by MEK and positive feedback[31-34].

However, in contrast to the linear response of the integrated pEGFR signal (Figure 2C), it can be observed from the time profiles for 25 and 50 ng/ml EGF trigger a nearly identical ppErk1/2 response (Figure 3B). This means that the ppErk1/2 response saturates for high ligand concentrations, and hence suggests that the MAPK cascade may limit the dynamic range of signal transmission.

Using DAPI staining to contour the nuclear regions also allowed us to determine the localization of ppErk1/2 inside the cell (Figure 3B). We found that the nuclear level of ppErk1/2 showed a similar time course as the cytoplasmic levels, but staining intensity of ppErk1/2 was higher in the nucleus than in the cytoplasm. This apparent amplification of the signal in the nucleus however could potentially be due to the bright field imaging, because cells are flattest at the cytoplasmic region and thus the cytoplasmic signal is integrated over a smaller volume than the nuclear signal.

Finally, to understand how each individual signalling stage contributes to signal transmission from the extracellular space to the nucleus, we integrated the ppErk1/2 response over time and deconvolved the EGF signalling data into three subsystems (Figure 4) the receptor subsystem, the MAPK cascade, and the nuclear import of active Erk1/2. Both the receptor and nuclear import display linear signal transmission, whereas the MAPK cascade introduces a saturable response. The input-output relationship of the complete system therefore displays saturation, which limits the cellular sensitivity to stronger EGF stimuli. This suggests that the nonlinear relationship between EGF concentration and cummulative nuclear ppErk1/2 results only from the dynamics of the MAPK cascade.

4 Conclusions

The link between growth factors and cellular responses depends on how extracellular signals are sensed and transmitted from the cell surface to the nucleus. In this article we used a modular approach to study how an EGF signal is transmitted by the EGFR system, the downstream MAPK signalling cascade, and the nuclear import of ppERK1/2. Our main finding is that the receptor system displays a linear input-output relationship between the ligand concentration and the cummulative receptor activation over time. We therefore conclude that the receptor system might act like a linear sensor, translating extracellular information proportionally into an intracellular signal.

Acknowledgments
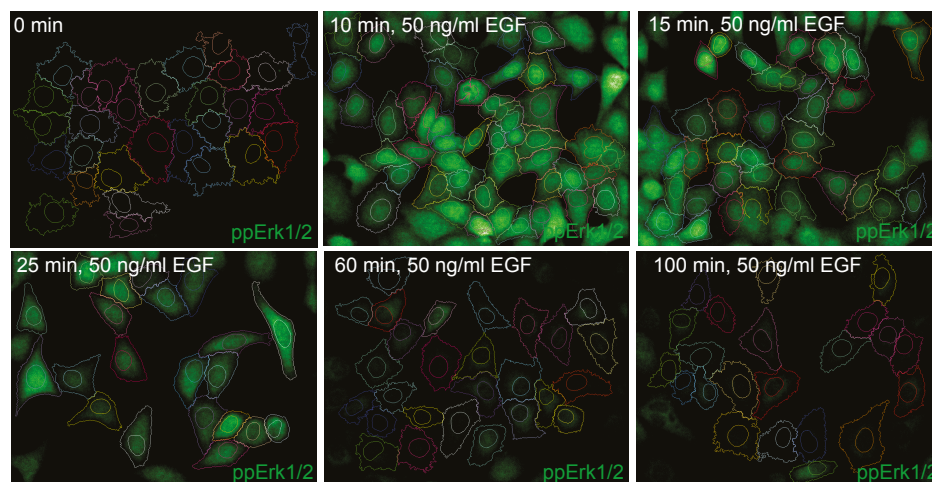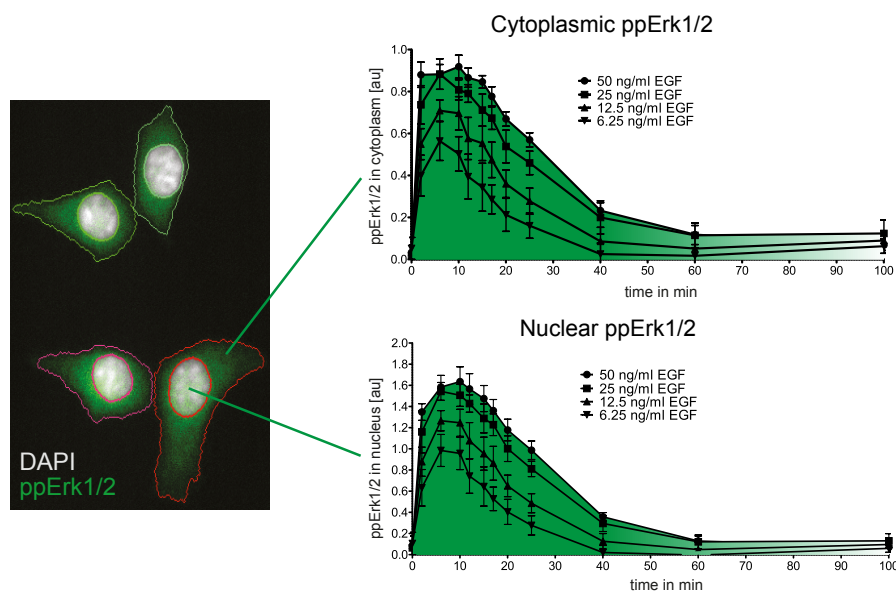
Fig. 3 Transient activation of ppErk1/2 after stimulation of Hela cells with different concentrations of EGF. **A)** Additionally to EGFR quantification as shown in Figure 2, ppErk1/2 (T185/Y187, T202/Y204) was quantified to investigate how the receptor signal is changed by downstream signalling. The measurements were obtained and normalized as described in Figure 2. **B)** To distinguish between cytoplasmic and nuclear levels of ppErk the nuclear area was contoured by DAPI staining as described in the Material and Methods section. Nuclear ppErk signals were normalized by dividing by the highest value for the cytoplasmic area to allow for a comparison of cytoplasmic and nuclear values.
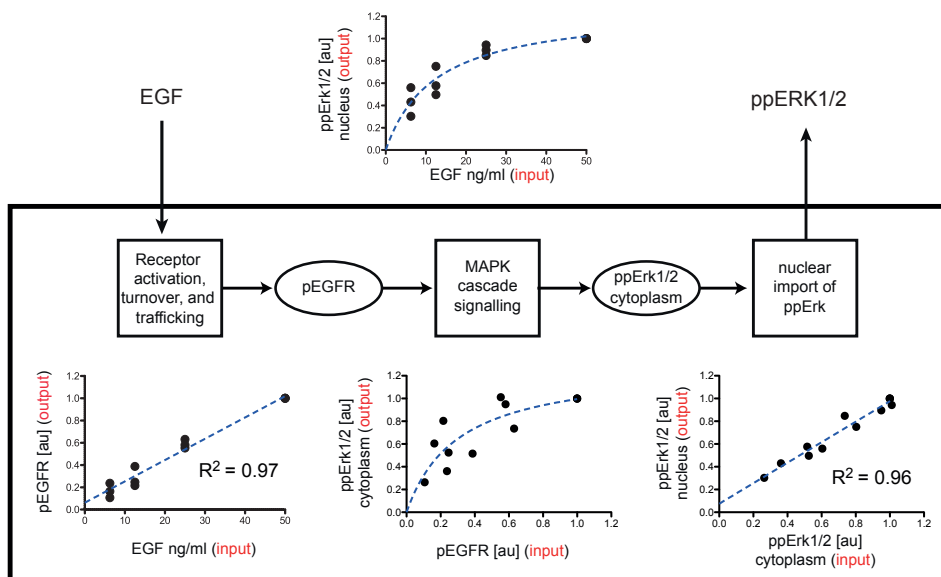
Fig. 4 Modular input-output description EGF signalling. Blocks represent subsystems and the arrows represent the signals interconnecting them. To determine the input-output relationship the integrals of the measured proteins are plotted against each other. Data points are individual biological replicates normalized to the highest value observed on one plate. Dashed lines are linear fits and the curves are Michaelis-Menten fits of the data.

References

1 R. Avraham and Y. Yarden, *Nat Rev Mol Cell Biol*, 2011, **12**, 104–117.

2 I. Dikic and S. Giordano, *Curr Opin Cell Biol*, 2003, **15**, 128–135.

3 G. Scita and P. P. Di Fiore, *Nature*, 2010, **463**, 464–473.

4 A. Sorkin and M. von Zastrow, *Nat Rev Mol Cell Biol*, 2002, **3**, 600–614.

5 H. Masui, L. Castro and J. Mendelsohn, *J Cell Biol*, 1993, **120**, 85–93.

6 K. Miller, J. Beardmore, H. Kanety, J. Schlessinger and C. R. Hopkins, *J Cell Biol*, 1986, **102**, 500–509.

7 A. M. Honegger, R. M. Kris, A. Ullrich and J. Schlessinger, *Proc Natl Acad Sci USA*, 1989, **86**, 925–929.

8 A. Citri and Y. Yarden, *Nat Rev Mol Cell Biol*, 2006, **7**, 505–516.

9 M. K. Nyati, M. A. Morgan, F. Y. Feng and T. S. Lawrence, *Nat Rev Cancer*, 2006, **6**, 876–885.

10 P. Gorden, J. L. Carpentier, S. Cohen and L. Orci, *Proc Natl Acad Sci USA*, 1978, **75**, 5025–5029.

11 H. T. McMahon and E. Boucrot, *Nat Rev Mol Cell Biol*, 2011, **12**, 517–533.

12 A. Sorkin and M. von Zastrow, *Nat Rev Mol Cell Biol*, 2009, **10**, 609–622.

13 H. S. Wiley and D. D. Cunningham, *Cell*, 1981, **25**, 433–440.

14 Shankaran, Resat and H. S. Wiley, *PLoS Comput Biol*, 2007, **3**, e101.

15 W. W. Chen, B. Schoeberl, P. J. Jasper, M. Niepel, U. B. Nielsen, D. A. Lauffenburger and P. K. Sorger, *Molecular Systems Biology*, 2009, **5**, 1–19.

16 K. A. Fujita, Y. Toyoshima, S. Uda, Y.-I. Ozaki, H. Kubota and S. Kuroda, *Science Signaling*, 2010, **3**, ra56.

17 P. Burke, K. Schooler and H. S. Wiley, *Mol Biol Cell*, 2001, **12**, 1897–1910.

18 Shankaran, H. S. Wiley and Resat, *BMC Syst Biol*, 2007, **1**, 48.

19 H. Resat, J. A. Ewald, D. A. Dixon and H. S. Wiley, *Biophys J*, 2003, **85**, 730–743.

20 V. Becker, M. Schilling, J. Bachmann, U. Baumann, A. Raue, T. Maiwald, J. Timmer and U. Klingmuller, *Science*, 2010, **328**, 1404–1408.

21 J. J. Hornberg, B. Binder, F. J. Bruggeman, B. Schoeberl, R. Heinrich and H. V. Westerhoff, *Oncogene*, 2005, **24**, 5533–5542.

22 R. Heinrich, B. G. Neel and T. A. Rapoport, *Mol Cell*, 2002, **9**, 957–970.

23 D. A. Oyarzún, F. López-Caamal, M. R. García, R. H. Middleton and A. Y. Weiße, *PLoS ONE*, 2013, **8**, e62834.

24 A. R. Asthagiri, C. A. Reinhart, A. F. Horwitz and D. A. Lauffenburger, *J Cell Sci*, 2000, **113 Pt 24**, 4499–4510.

25 M. Rojas, S. Yao and Y. Z. Lin, *J Biol Chem*, 1996, **271**, 27456–27461.

26 H. S. Wiley, S. Y. Shvartsman and D. A. Lauffenburger, *Trends Cell Biol*, 2003, **13**, 43–50.

27 K. Roepstorff, L. Grøvdal, M. Grandal, M. Lerdrup and B. van Deurs, *Histochem Cell Biol*, 2008, **129**, 563–578.

28 A. Kirisits, D. Pils and M. Krainer, *Int J Biochem Cell Biol*, 2007, **39**, 2173–2182.

29 C. C. Reddy, A. Wells and D. A. Lauffenburger, *Biotechnol Prog*, 1994, **10**, 377–384.

30 Y. Mosesson, G. B. Mills and Y. Yarden, *Nat Rev Cancer*, 2008, **8**, 835.

31 A. Goldbeter and D. E. Koshland, *J. Biol. Chem.*, 1984, **259**, 14441–14447.

32 C. Y. Huang and J. E. Ferrell, *Proc. Natl. Acad. Sci. U.S.A.*, 1996, **93**, 10078–10083.

33 G. C. Brown, J. B. Hoek and B. N. Kholodenko, *Trends Biochem. Sci.*, 1997, **22**, 288.

34 J. E. Ferrell and E. M. Machleder, *Science*, 1998, **280**, 895–898.

35 R. Fritsche-Guenther, F. Witzel, A. Sieber, R. Herr, N. Schmidt, S. Braun, T. Brummer, C. Sers and N. Blüthgen, *Mol Syst Biol*, 2011, **7**, 1–13.

36 C. Y. Huang and J. E. Ferrell, *Proc Natl Acad Sci USA*, 1996, **93**, 10078–10083.

37 O. E. Sturm, R. Orton, J. Grindlay, M. Birtwistle, V. Vyshemirsky, D. Gilbert, M. Calder, A. Pitt, B. Kholodenko and W. Kolch, *Science Signaling*, 2010, **3**, ra90.